The 2013 World Congress on
Advances in Structural Engineering and Mechanics (ASEM13)
Jeju, Korea, September 8-12, 2013

Wireless Sensor Networks for Monitoring and Control of Frame Structures

*Markus Zellhofer[1)], Albert Poetsch[2)], Georg Moestl[3)] and Michael Krommer[4)]

[1,2)] Austrian Center of Competence in Mechatronics (ACCM), A-4040 Linz, Austria
[3)] Institute for Integrated Circuits, Johannes Kepler University, A-4040 Linz, Austria
[4)] Institute for Technical Mechanics, Johannes Kepler University, A-4040 Linz, Austria
[1)] markus.zellhofer@accm.co.at

ABSTRACT

Distributed piezoelectric actuators and sensors are well suited for monitoring and control of flexible structures. Sensors are designed such that their output measures specific kinematical entities (e.g. the deflection of a floor of a frame structure) or to detect and locate damage. Concerning the latter topic of damage monitoring nilpotent sensors, which have a trivial signal for an undamaged structure, but which result into a non-trivial signal in case damage occurs, can be used. As in practice continuously distributed sensors are approximated by networks of piezoelectric sensor patches, multi-purpose sensor networks can be put into practice and used for different monitoring tasks. The continuous distribution is approximated by proper weight assignment and superposition of the patch sensor signals.
In order to enable monitoring of spacious and complex structures embedded, low cost, and energy efficient wireless communication systems appear to be an important, yet critical solution. Wireless sensor nodes, to which the sensor patches are wired, are positioned on local subareas of the monitored structure. To reduce the amount of data to be transmitted, at each sensor node the digitalized signals from the piezoelectric patches of the substructure are preprocessed and properly truncated to a signal with the meaning of a specific kinematical entity of the substructure. A base station collects the data of the distributed sensor nodes in a synchronized manner and further processes these truncated signals. For closed-loop applications the wireless communication between the base station and the sensor nodes must be bi-directional and robust. Using spatial collocation between the sensor network and an additional actuator network the monitored kinematical entity can be controlled; this is also true, if the latter entity is correlated with damage by using nilpotent sensor and actuator networks.

[1)] Junior Researcher
[2)] Junior Researcher
[3)] Junior Researcher
[4)] Associate Professor

In the present paper first steps of the application of the described approach for the monitoring and control of a three-storey frame structure by piezoelectric sensor and actuator networks with an implemented wireless communication system are presented. Important concepts of both, the mechanical sensor networks and the wireless communication system are discussed and first experimental verification results on an elastic member of the frame structure are included in the paper.

1. INTRODUCTION

Frame structures are very common representatives for lightweight structures in civil and mechanical engineering. For structures in critical environment, one can be interested in nondestructive, continuous monitoring of them. Strain-type sensors require less space and can be integrated into the materials the monitored structures are built-on. Especially, this is correct for modern materials (e.g. carbon fibre laminate), where the sensor materials can be embedded in the layers during fabrication. In this paper piezoelectric ceramics are used not only for the strain sensor network but also for actuation in terms of an eigenstrain actuation, which will be collocated to the sensor signal. The importance of collocation between actuation and sensing for closed-loop control applications has been shown by Kugi (2001). In case of networks of sensors and actuators, a connection by wires is possible for compact parts and substructures. For spacious structures it seems necessary to divide the structures into parts and substructures where the connection is done by wires, while the connection between the substructures is realized by a wireless communication system. First steps on the integration of mechanical sensor networks and wireless connected sensor nodes are discussed in this paper. Earlier work on structural health monitoring by means of wireless sensor networks can be found in (Kim 2007) and (Hackmann 2010), for example. Using wireless systems allows the monitoring task on the distributed mechanical system at a much lower price and in a decreased invasive manner, so the functionality of the system is less affected. A general survey about the motivation for the use of wireless networks for supervising structural health can be found in (Pin 2010) and in (Gaudenzi 2013). A logical development step is to apply wireless sensor networks to the monitoring path of closed-loop control systems and to extend the wireless link to drive the actuators. Compared to a wired network this creates new challenges regarding the latency of the sensor and actor signals. Unfortunately, the problem complexity becomes overwhelming as besides latency there are tight constraints regarding high precision data, high frequency sampling, time synchronized sampling, large-scale networks, and reliable data collection. We therefore reduce complexity by means of breaking down the mechanical system to a single beam and focus on the latency constraint on the monitoring path of the system. However, in our opinion, this is the first step to extend the concept of wireless structural health monitoring to wireless closed-loop controlled structural systems.

2. PIEZOELECTRIC SENSORSFOR SMART BEAMS

To derive the sensor equation for a piezoelectric strain-type sensor we refer to (Irschik 1998) and (Krommer 2001)and derive the electric equations in a piezoelectric layer from the Maxwell Equation

$$div\mathbf{D} = 0 \tag{1}$$

where $\mathbf{D}$ is the electric displacement vector acting in the volume V . The electric potential $\phi(x,y,z) = \phi(z)$ for a thin, ideally electroded layer is assumed to be only a function of the thickness direction of the layer. Due to the relation for the electric field components $E_i = -\partial\phi / \partial i$ and the previous assumption, the in-plane components of the electric field on the electrodesand the electric displacements in the ceramic $D_x = D_y = 0$ vanish. Comparing to (Miu 1993) the electric displacement in a linear dielectric, polarizable media turns out to be constant over the thickness direction $dD / dz = 0$. Finally we find

$$D_z = \eta_{33}(E_z - \bar{E}_z) = \frac{1}{h_p}\int_{z_1}^{z_2} D_z dz = \frac{1}{h_p}\int_{z_1}^{z_2} \eta_{33}(E_z - \bar{E}_z)dz = \eta_{33}\frac{V}{h_p} - \eta_{33}\frac{1}{h_p}\int_{z_1}^{z_2} \bar{E}_z dz \tag{2}$$

with. The electric eigenfield due to the direct piezoelectric effect $\bar{E}_z$ depends on the axial strain for the beam theory.

$$\bar{E}_z = \frac{e_{31}}{\eta_{33}}\varepsilon_{xx} \tag{3}$$

From the previous relation for the electric displacement we find the electric charge by utilizing Gauss law of electrostatics, where the hull integration reduces to the integration over the area of the electrodes.

$$A_{el} = \int_L S_{el} dx \tag{4}$$

The relation for the electric charge reads:

$$Q = \int_{A_{el}} D_z dA = \frac{\eta_{33} A_{el}}{h_p} V - \frac{\eta_{33}}{h_p}\int_L S_{el}\int_{z_1}^{z_2} \bar{E}_z dz dx = C_p V - \frac{e_{31}}{h_p}\int_L S_{el}\int_{z_1}^{z_2} \varepsilon_{xx} dz dx \tag{5}$$

is a shape function which represents the width of the piezoelectric layer. Equation (5) is already the sensor equation for the piezoelectric layer on a smart beam for undefined electrical conditions on the electrode. In the following the short circuit electrodes mode is used, where the electrical voltage vanishes in the sensor equation and the total charge on the electrodes emerges to the sensor signal.

$$Q(t) = y(t) = -\frac{e_{31}}{h_p}\int_L S_{el}(x)\int_{z_1}^{z_2} \varepsilon_{xx} dz dx \tag{6}$$

For a Bernoulli-Euler beam in pure bending the strain reduces to a function of the linearized curvature of the neutral axis of the beam.

$$\varepsilon_{xx} = -zw_0'' \text{ with } (\,)'' = \frac{d^2}{dx^2} \tag{7}$$

With $z_m = (z_1 + z_2)/2$ the sensor signal becomes:

$$Q(t) = y(t) = -\frac{e_{31}}{h_p}\int_L S_{el}\int_{z_1}^{z_2}(-zw_0'')\,dz\,dx = e_{31}z_m\int_L S_{el}w_0''\,dx \tag{8}$$

To find a mechanical interpretation of the sensor signal the principle of virtual work is applied to the quasi static state of equilibrium of an auxiliary system probably derived by releasing constraints of the smart beam.

$$\delta W = \delta W^i + \delta W^a = \int_L (M^{qs(p_z)}\,\delta w_0'')dx + \int_L (p_z^{qs}\,\delta w_0)\,dx = 0 \tag{9}$$

The virtual deflection has to fulfill the boundary conditions, or with other words, to be kinematically admissible. Obviously the actual deflection is an aspirant to be used for the virtual deflection and the expression for the virtual work becomes:

$$0 = \int_L (M^{qs(p_z)}w_0'')dx + \int_L (p_z^{qs}w_0)dx \tag{10}$$

Comparing equations (8) and (10) one can choose the shape function proportional to the quasi static bending moment due to a lateral external quasi static force distribution.

$$S_{el} = \frac{M^{qs(p_z)}}{e_{31}z_m} \tag{11}$$

The sensor signal than becomes correlated to the work conjugate of the applied force on the original system.For example, one can load the tip of a smart cantilever with a single unit force in lateral direction to calculate the shape function from the bending moment due to this tip load. Therefore the sensor signal correlates with the lateral tip deflection. For redundant structures, shape functions can be found, where the sensor signal is vanishing for any deformation of the beam axis, until the monitored structure is changing its kinematical behaviour due to failure. This type of sensor is a proper candidate for structural health monitoring. For the design of a so called nilpotent sensor or compatibility sensors of redundant structures, the quasi static bending moment distribution,due to statically indeterminate single forces and moments acting on positions where kinematically constraints are released, can be found by the well-known force method, see e.g. (Ziegler 1998). The nilpotent sensor signal for any time fulfils:

$$y(t) = e_{31}z_m\int_L S_{el}w_0''dx = 0 \tag{12}$$

3. PIEZOELECTRIC ACTUATORS FOR SMART BEAMS

Refering to (Tauchert 1992) and (Irschik1998) the axial strain in the piezoelectric layer affected by piezoelectric based eigenstrainreads: $\bar{\varepsilon}_{xx} = d_{31}E_z = e_{31}S_{11}E_z$

$$\varepsilon_{xx} = S_{11}\sigma_{xx} + S_{12}\sigma_{yy} + S_{13}\sigma_{zz} + d_{31}E_z \tag{13}$$

For slender beams this relation can be reduced due to the predomination of the axial stress and reformulated to

$$\sigma_{xx} = \frac{1}{S_{11}}(\varepsilon_{xx} - \bar{\varepsilon}_{xx}) \tag{14}$$

Inserting a conversion of equation (2) into the relation for the eigenstrain leads to

$$\bar{\varepsilon}_{xx} = \frac{e_{31}}{S_{11}}(\frac{V}{h_p} + \bar{E}_z - \frac{1}{h_p}\int_{z_1}^{z_2}\bar{E}_z dz) \tag{15}$$

Integration of equation (14)over the total cross section of a beam existing of N layers where the kth piezoelectric layer is acting, leads to a stress resultant which represents the bending moment on the beam level.

$$M_y = \sum_{k=1}^{N}\int_{A^k}\sigma_{xx}^k z dA = \sum_{k=1}^{N}\int_{A^k} Y^k(\varepsilon_{xx} - \bar{\varepsilon}_{xx}^k) z dA \tag{16}$$

As in the previous section the Bernoulli-Euler beam assumption for the strain is used.

$$\varepsilon_{xx} = -zw_0'' \tag{17}$$

After inserting equation (17) into equation (16)the equation for the bending moment results into:

$$M_y = -\bar{D}w_0'' - \bar{M} \tag{18}$$

$\bar{D}$ representthe bending stiffness which is influenced by piezoelectric coupling.

$$\bar{D} = \sum_{k=1}^{N}\int_{z^{k-1}}^{z^k} b^k(\frac{1}{S_{11}^k}z^2 + \frac{d_{31}^k e_{31}^k}{\eta_{33}}z^2 - \frac{d_{31}^k e_{31}^k}{\eta_{33}}z_m^k z)dz \tag{19}$$

$z_m^k = (z^k + z^{k-1})/2$ is the distance of the middle plane of the piezoelectric layer to the neutral axis of the beam. The term $\bar{M}$ provides the actuating bending moment due to an applied electrical voltage on the electrodes of the kth -layer.

$$\bar{M} = \sum_{k=1}^{N}\int_{z^{k-1}}^{z^k}\frac{b^k}{h^k}e_{31}^k V^k z dz \tag{20}$$

As for the sensor equation, the shape function of the piezoelectric actuating layer plays an important role. For such layers the width b^k becomes

$$b^k = S_{el}^k \tag{21}$$

Irschik (Irschik2003) proposed a method where the Green's function in context with the reciprocal theorem of Bettican be used to find a proper shape function for dynamic shape control. This theorem extended with respect to the influence of eigenstrains is also called Maysel's formula (Ziegler 1998).The dynamic shape control problem provides a solution for the question: How should a shape function of a piezoelectric layer be chosen for the elimination of the deflection of a smart beam, due to a known dynamic external force loading in time and space, by means of a feed-forward control?The reciprocal theorem is

$$1 \cdot w_0(\xi) = \int_L \frac{(M^{qs,(p_z)}(x) + \bar{M}(x))M^d(x,\xi)}{\bar{D}} dx \tag{22}$$

where $M^d(x,\xi)$ denotes the bending moment due to a single dummy force at the varying location ξ. The relation holds for static problems as well as dynamic ones; for the latter, the integral must be understood as a convolution integral. $\bar{M}$ and $\bar{D}$ are the actuation moment and the bending stiffness for an smart beam with piezoelectric layers which following directly from equations (19) and (20). One can see directly from equation (22) that the total deflection in lateral direction is vanishing if the following equation is satisfied:

$$M^{qs,(p_z)}(x) + \bar{M}(x) = 0 \tag{23}$$

From equation (23) thebending actuator shape function for the kth layer, actuating solely on a smart beam, becomes:

$$S_{el}^k = \frac{M^{qs(p_z)}}{e_{31}^k z_m^k} \tag{24}$$

For redundant structures also the concept of nilpotent actuation is introduced in the literature, see (Irschik1998). Nilpotent actuators do not induce any deformation in the system until its kinematical constraints changes. This seems to be a very powerful concept in combination with collocated nilpotent sensing in the context of structural health control.

4. COLLOCATION OF ACTUATORS AND SENSORS

Comparing equations (11)and(24) of sensor and actuator shape functions,the equality of the shape functions is pointed out and advantages for application arises. First of all, it is sufficient to design only one shape function, for the actuator or the sensor. A further advantage of,so called,collocated sensors and actuators is given for the application as self-sensing actuators, where sensing and actuation is done by one device. By referring to the power theorem of mechanics (Ziegler 1998, Chadwick 1976),collocation turns out, as the power of the actuation is equal to the time derivative of the sensor-signal multiplied by the time variation of the actuation. For example see

also (Krommer 2004). To derive the relations for collocation, exemplarily one can begin with the differential equation for the Bernoulli-Euler beam in pure bending.

$$M_y'' + p_z = \bar{P}\ddot{w} \quad (\,)'' = \frac{d^2}{dx^2} \quad \dot{(\,)} = \frac{d^2}{dt^2} \tag{25}$$

Inserting the equation for the bending moment from equation (18)into(25), multiplying the resulting equation by the time derivative of the deflection $\dot{w}$ and integrating over the span of the beam, results into the theorem of power for the smart beam.

$$\int_L ((\bar{D}w'')'' + \bar{P}\ddot{w})\dot{w}dx = \int_L (p_z - \bar{M}'')\dot{w}dx$$

Integration of the terms with the bending stiffness $\bar{D}$ and the actuation moment $\bar{M}$ twice by parts and considering the bending stiffness and the effective inertia mass $\bar{P}$ as constant in time and space leads to:

$$\begin{aligned} &\frac{d}{dt}\int_L \frac{1}{2}(\bar{D}w''w'' + \bar{P}\dot{w}\dot{w})dx = \int_L p_z\dot{w}dx - \int_L \bar{M}\dot{w}''dx \\ &\frac{d}{dt}(W+T)dx = L^e + L^a \end{aligned} \tag{26}$$

$(W+T)$ is the sum of the elastic part of the strain energy W and the kinetic energy T. L^e and L^a are the power of the external forces and the power of the piezoelectric actuation; the latter can be written as:

$$L^a = -\int_L \bar{M}\dot{w}''dx = V\cdot(-e_{31}z_m\int_L S_{el}\dot{w}''dx) = u\cdot(-\dot{y}) \tag{27}$$

From a closed loop control point of view, Kugi(Kugi 2001) has shown the importance of this concept in the framework of Port Controlled Hamiltonian Systems. The closed loop system gets stable and observation / actuation spillover is avoided.

5. SENSOR/ACTUATOR NETWORKS FOR FRAMESTRUCTURES

So far the sensor and actuator shape functions have been considered continuously distributed. Deriving from former results, see (Krommer 2010), the sensor signal for a frame structure with sidewalls, modelled as Bernoulli-Euler beams and connected by m rigid floors reads.

$$y = \sum_{i=1}^{m}\left(\int_{H_i} S_{iL}w_{iL}''dx_{iL} + \int_{H_i} S_{iR}w_{iR}''dx_{iR}\right), \; (\,)'' = \frac{\partial^2}{\partial x_{i(L,R)}^2} \tag{28}$$

The subscripts L and R refer to the left or right sidewall of the frame structure. H_i is the corresponding height of the flexible sidewall.In practice it is more feasible to discretize the distributed shape function due to equal piezoelectric ceramic patches. Commercially available ceramic patches embedded in polymers with contacted electrodes are used in this contribution.These patches are span-wise constant and have to be placed properly over the beam-type structure and weighted individually. For this task the individual sidewall has to be considered as divided into n subsections of dimension $[x_{ij}, x_{ij}+\Delta\bar{x}]$ with $j=1..n$, $x_{i1}=0$ and $x_{in}=L$. Each patch is placed within one subsection in the span . The sensor signal for the $[\bar{x}_{ij}, \bar{x}_{ij}+\Delta\bar{x}]$ network of piezoelectric patches, approximating the distributed sensor signal depends on the individual weight and position for each piezoelectric patch.

$$\bar{y}=\sum_{i=1}^{m}\sum_{j=1}^{n}\left(S_{ijL}\int_{\bar{x}_{ijL}}^{\bar{x}_{ijL}+\Delta\bar{x}} w''_{iL}\,dx_{iL}+S_{ijR}\int_{\bar{x}_{ijR}}^{\bar{x}_{ijR}+\Delta\bar{x}} w''_{iR}\,dx_{iR}\right) \tag{29}$$

To minimize the error function $\bar{e}=y-\bar{y}$ the weights $S_{ij(L,R)}$ and position $\bar{x}_{ij(L,R)}$ have to be determined by approximating the original distributed bending moment due to the external load, by considering applied single forces and moments on the interfaces between the subsections. In case of exact approximation of the distributed bending moment the error function vanishes for the relations:

$$\bar{x}_{ij(L,R)}+\frac{1}{2}\Delta\bar{x}=\left(\int_{x_{ij(L,R)}}^{x_{ij(L,R)}+\Delta x}\frac{S_{i(L,R)}(x_{i(L,R)})}{D(x_{i(L,R)})}dx_{i(L,R)}\right)^{-1}\int_{x_{ij}}^{x_{ij}+\Delta x}\frac{S_{i(L,R)}(x_{i(L,R)})}{D(x_{i(L,R)})}x_{i(L,R)}\,dx_{i(L,R)} \tag{30}$$

$$S_{ij(L,R)}\bar{D}=\frac{1}{\Delta\bar{x}}\int_{x_{ij(L,R)}}^{x_{ij(L,R)}+\Delta x}\frac{S_{i(L,R)}(x_{i(L,R)})}{D(x_{i(L,R)})}dx_{i(L,R)},\quad i=1,...,m\ \ \mathrm{j}=1,...,n \tag{31}$$

According to (Irschik 2009) and Huber (Huber 2011)relations(30) and (31)to determine the weight and the center-position of the ith patch, exist, where D is the bending stiffness of the beam and $\bar{D}$ is the bending stiffness of the coupled smart beam represented by equation (19). (30)and(31) leads to a system of $4mn$ equations for determining the $4mn$ indeterminate weights and positions. In case of multi-purpose networks the position of the individual patches are fixed beforehand, than the $2mn$ indeterminate weights are calculated by a least square algorithm.

6. WIRELESS COMMUNICATION SYSTEM – IMPLEMENTATION

In this section we present the implementation of the wireless communication system, i.e., which hardware and software components are used and how they interact. Several design decisions based on physical quantities like sampling rate, resolution, communication datarate, etc must be made. These constraints are given by the

mechanical system on the one hand and by the software and hardware on the other hand. As this is a prototype we use off-the-shelf available hardware from Texas Instruments.

6.1 System Overview

To reduce design complexity we first implement the wireless sensor network at one elastic member of the three-storey frame structure comprising three piezoelectric sensors and three piezoelectric actuators. Given this simplified scenario, we designed a point to point wireless communication system consisting of one wireless sensor node wired to three piezoelectric sensor-patches, and one base station which forwards the received sensor data to a DSpace-system, which processes this data. If the DSpace-system does not perform an algorithm for e.g. stabilizing the mechanical structure but is only monitoring the structure, the piezoelectric actuators are not needed. The wireless system comprises components to enable proper signal conditioning of the analog signals.

Each piezoelectric sensor patch is hooked up to a charge amplifier, which delivers a voltage output level which reflects a weighted integral over the strain the piezoelectric patch suffers. This analog signal is the input of the wireless communication system. As a first step this voltage level is digitalized bythe help of an Analog to Digital Converter (ADC). We choose the ADS8638 ADC from Texas Instruments which supports up to 8 bipolar input channels at 12 bit of resolution, a maximal sampling rate of 1 million samples per second. Further, different input voltage level ranges are supported, which offers a flexible interface for converting such high dynamic output range signals that occur at piezoelectric sensors. Given the ± 1 V output level of the charge amplifier, we use the ± 2.5 V symmetric voltage range of the ADC. An optional channel sequencing mode allows for an efficient hardware assisted conversion of more than one channel, which is a useful feature when all three piezo-patches are connected and can be sampled almost simultaneous.

The ADC is controlled by a proprietary software stack running on a MSP430F5438A microcontroller unit (MCU). Low level drivers were implemented, utilizing the serial peripheral interface (SPI) of the ADC, for efficient configuration and sampling of the ADC. The microcontroller comprises a 16 bit RISC architecture and 256 KByte of flash memory. Supported clock frequencies range from 32 KHz up to 25 MHz and enable in combination with different low power modes energy efficient processing or high performance processing. Further, the microcontroller comprises internal blocks like serial interfaces, 16 bit timers, direct memory access, etc. Although, an internal ADC is also available we use an external one because of higher performance and the need of converting a signal with symmetric voltage range, which is not possible with the internal ADC without an additional electric circuit.

For the purpose of wireless communication we selected the CC2500 radio transceiver. The CC2500 is a packet-oriented, low-cost, and energy efficient radio transceiver which enables datarates of up to 250 Kbits per second in the 2.4 GHz ISM band. It supports intensive hardware support for e.g. automatic Clear ChannelAssessment (CCA) used for collision free communication, data buffering and link quality indication.In our first prototype the CC2500 is controlled by the SimpliciTInetwork stack from Texas

Instruments running on the MCU, utilizing a SPI interface. SimpliciTI is a network stack targeting low power and low datarate radio transceivers which are organized in point to point connections, in a star topology, or in a mesh network.
The base station comprises a Digital to Analog Converter (DAC) which allows a seamless integration of the wireless communication system into the well establishedDspace control system. By still using the analog input channel of the Dspace system an easy replacing of the wired connection to the output of the charge amplifier is possible. Although converting a already digitized signal back to an analog signal degrades the signal to noise ratio (SNR) a second reason for using the analog input of the Dspace system instead of a digital interface (e.g. RS232) during the prototype phase is the decoupling of the sampling frequency of the wireless communication system and the cycle time of the controller algorithm running inside Dspace.In a future step the DAC can be removed by directly forwarding the digitized data from the base station to a digital interface of the Dspace system if the impact of having two different cycle times is more clear. The DAC is a AD5752 with 16 bit resolution supporting several ouput voltage levels and is controlled by the MCU of the base station via an SPI interface.

6.2Design Questions and Results

Integration of the whole system in a closed-loop scenario rises two fundamental design questions, namely, (i) what is the maximum latency of the system, and (ii) what is the required and achieveable sampling rate of the system. These questions are non-trivial, as the mechanical and the wireless communication system must be considered.
To answer the first question, we divided the wireless communication system in three parts and measured the latency of each part by means of pin toggling events. We toggled the voltage level of a digital I/O pin of the microcontroller (sensor node and base station) and measured the time with an oscilloscope. The corresponding software initializes the action given in Table 1, and therefore stated values include execution time of the software running on the microcontroller, and processing time of the external hardware. After the first measurements of the system were taken we made some optimizations of the system to minimize the latency. Optimizations comprised increasing the clock frequency of the microcontroller to 16 MHz, clocking the ADC and DAC with a high frequency clock (i.e., submaster clock of the microcontroller), and modify the SimpliciTIradio network stack. SimpliciTI per default calibrates the radio transceiver before a packet is sent. This calibration phase lasts for several microseconds and is not always needed. We therefore changed the stack to calibrate just at every fourth transmission. Further, we deactivated the CSMA/CA algorithm of the stack and the corresponding back-off algorithm. As we plan to organize the sensor nodes in a time division multiple access scheme (TDMA), where every sensor node gets a dedicated time slot to send its data, the time-consuming CSMA/CA algorithm is no longer needed. As shown in Table 1we reduced the latency of the whole chain of the wireless communication from 5.77 ms to 1.958 ms.

Table 1: Measured latency for several actions of the original system and after optimizations.

Component	Unoptimized	Optimized
ADC – trigger conversion + conversion + readback	1.891 ms	0.153 ms
Radio – trigger sending + sending + reception	2.872 ms	1.727 ms
DAC – triggerconversion + conversion	1.281ms	0.078 ms

Results given in Table 1 are also relevant for the second question – what is the required and achievable sampling rate of the system.
The minimal sampling frequency is dictated by the eigenvalues of the mechanical system itself, according to the Nyquist theorem. In our case of a very inert and slow mechanical system this is not a big constraint. The maximum sampling rate achievable using a wireless communication system is dependent on the maximum data throughput which in turn is a function of the acquisition speed of the ADC, the over-the-air data rate of the transceiver, the processing speed of the microcontroller and the converting speed of the DAC. This parameters are also reflected by the latency and therefore gives also a upper limit for the sampling frequency. Sampling rates > 100 Hz has shown to give good results for the mechanical system. We decided to sample the beam with a sampling rate of 500 Hz using a 2-Byte datatype for each sample, which is within the achievable limits of the used wireless system. To ensure exact equidistant sampling, a major request in closed-loop theory, we use one internal timer of the microcontroller to sample the ADC every 2 ms. The sampling is implemented as an atomic section, i.e. as a corresponding interrupt service routine with disabled nested interrupts.

7. EXAMPLE

To monitor and control damage of the three storey frame structure, first of all, proper sensor and actuator networks have to be designed. Figure 1 shows the design of the distributed nilpotent sensor shape functions in four steps. In step 1 the original and nine times redundant frame structure can be seen. To derive the bending moment distributions which equals to the nilpotent sensor/actuator shape functions we release nine kinematical constraints until the structure is statically determinate. In this example the three storey frame will be considered as 3 three hinged arches stacked on top of each other. For this auxiliary structure we introduce statically indeterminate moments at the location of the released constraints, as proposed by the force method and calculate the bending moment distribution for each indeterminate moment.In step3 one of the nine linear independent bending moment distributions can be seen. Without further optimization the value of the indeterminate moment can be set to 1. The resulting nine distributed shape functions are not unique, because the choice of the released constraints is not unique. By linear combination of the nine shape functions nine new ones can be calculated. The simplest shape functions and less distributed ones due to

this procedure are shown in step 4. In each storey one nilpotent shape function is illustrated, which exists also for the other storeys. Because of the assumption of rigid bars the shape functions in the floors will be neglected. The marked nilpotent shape function will be used for the structural control of damage in this example. In case of a hinge in the elastic member of the frame structure this nilpotent sensor shape function measures the relative slope at the appearinghinge.

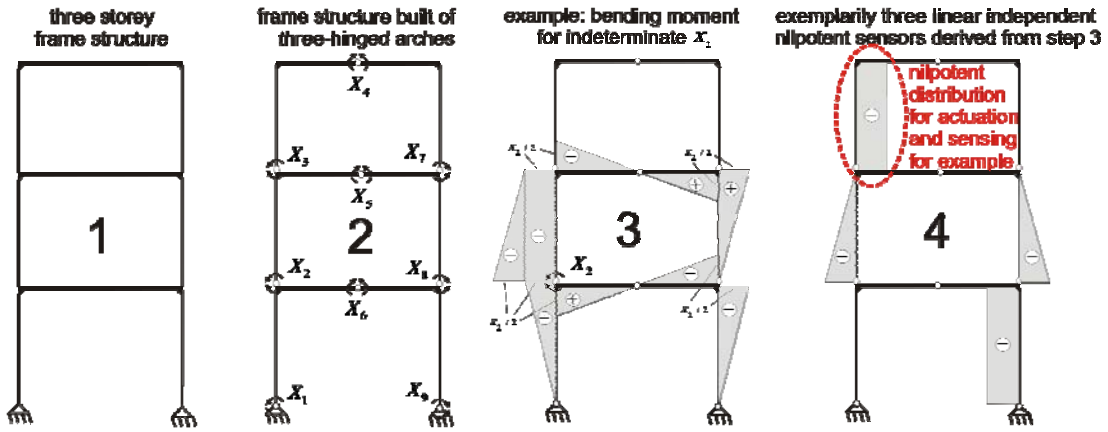

Figure 1: Four steps for deriving sensor and actuator distributions

The distributed shape functionsare approximated by three equal rectangular piezoelectric patches in each sidewall of the structure. The weights and positions are calculated by equations (30)and (31). In step 4 of Figure 1 the distributed shape functions depends only on linear and constant shape function. Therefore the results for the weighted sensor network can be seen in Figure 2. The required measurements of the real setup, needed for the calculation of the individual patch weights, will be introduced in the next section. The material parameters of the piezoelectric ceramics are given by the manufacturer.

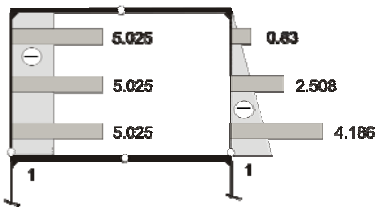

Figure 2: weights for sensor/actuator networks

Figure 3 shows the control scheme of the three storey frame structure. For the damaged structure, a hinge is introduced on the left sidewall of the third floor. The goal is the annihilation of this hinge due to active control. Sensor networks are attached on the entire frame structure for general monitoring of the frame structure. The damaged elastic member is additionally equipped with a collocated actuator network. For a first glimpse on the function of the control, the sidewall is extracted from the entire frame structure and is supported as cantilever. The wireless communication system (WCS) has unidirectional communication between sensor node and base node. The latter is connected to the actuator network, via a proper amplifier, by wires.

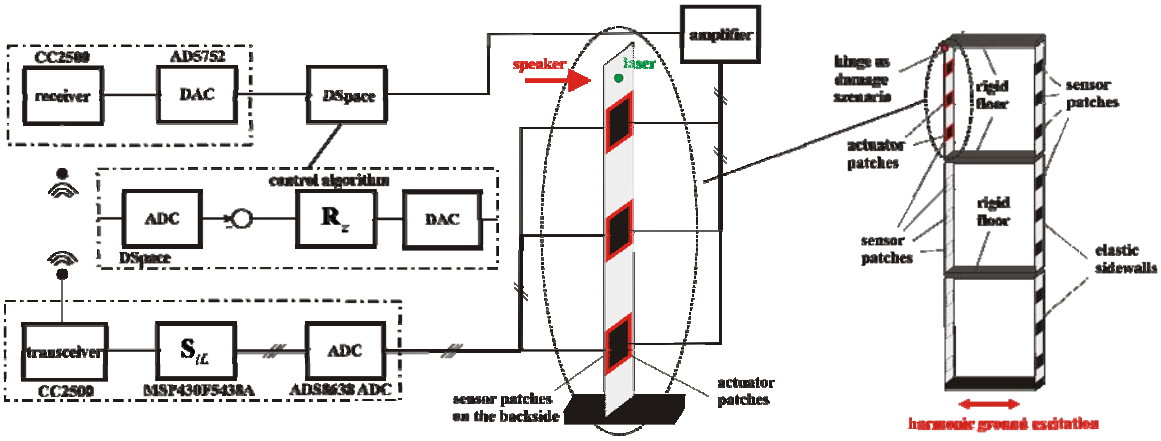

Figure 3: Control scheme with WSN for the elastic member of the frame structure

The piezoelectric sensor network is connected via charge amplifiers to the sensor node of the WCS. At the sensor node the setting of the individual sensor weights is possible. In the DSpace system the sensor feedback and the control algorithm are realised. The excitation of the beam happened by a bass speaker in the frequency domain of the first two eigenfrequencies. The deflection of the cantilever beam is measured by a laser sensor. The realised sensor/actuator distribution in this sidewall is the constant one, because of the interest in controlling the relative slope on the top of the beam. Therefore the sensor signal correlates with the latter. Especially for the first eigenfrequency, a qualitative comparison of the deflection signal from the laser sensor with the relative slope signalfrom the sensor network seems sufficient.

8. LABORATORY SETUP AND RESULTS

In Figure 4 the laboratory setup is shown. The dimensions of the beam are $L \times W \times T = 0.42\text{m} \times 0.04\text{m} \times 0.004\text{m}$ and the measurements of the three piezoelectric ceramics are $\Delta\bar{x} \times b \times h_p = 0.05\text{m} \times 0.03\text{m} \times 0.0005\text{m}$. The center positions for the ceramics are $\bar{x}_1 + \Delta\bar{x}/2 = L/6$, $\bar{x}_2 + \Delta\bar{x}/2 = L/2$ and $\bar{x}_3 + \Delta\bar{x}/2 = 5L/6$. In Figure 4 the elastic

sidewall of the frame structure with the sensor network on the upper side can be seen. The cantilever is clamped on the right side. On the left side the speaker for actuation and the laser sensor can be seen. For stronger actuation, on the lower side, two ceramics symmetric to the center positions of the sensor patches are applied and connected parallel, working as one actuator. The used ceramics are of type PIC 255. The weights for the actuator network are set to one because the magnification will be done by the control algorithm.

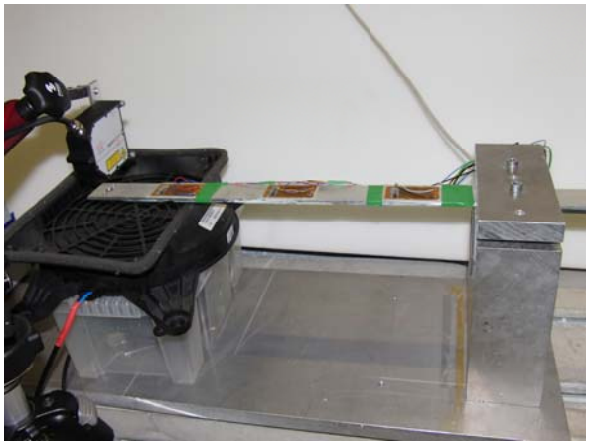

Figure 4: Laboratory setup

The open loop transfer function of the System $G(z)$ has been identified and is illustrated in Figure 5 in the q-domain which is necessary for the design of the control transfer function for time discretized system according to the sample rate of the controller. The open loop transfer function for controller and system $G\#(q)\cdot R\#(q)$ is designed by the method of loop shaping, e.g. see Nader (Nader 2008).

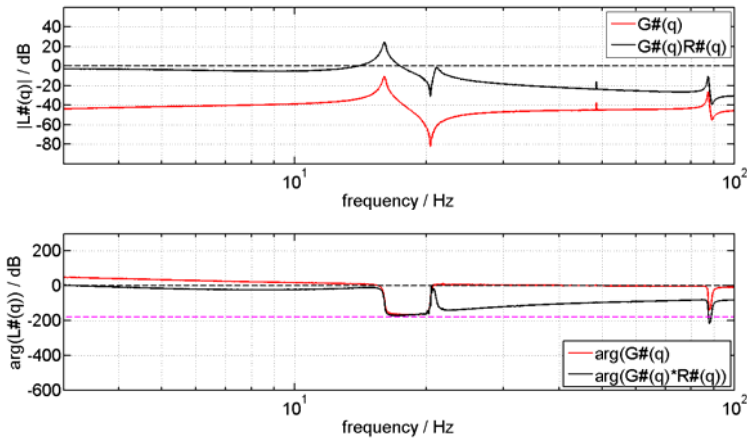

Figure 5: Transferfunction of the open loop

The first two eigenfrequencies are $f_1 \approx 16Hz$ and $f_2 \approx 94Hz$. In Figure 6 the relative slope on the tip of the cantilever measured by the sensor network can be seen. The magnification in the frequency spectrum reduces at the first eigenfrequency about 60dB and at the second eigenfrequencyat about 20dB .

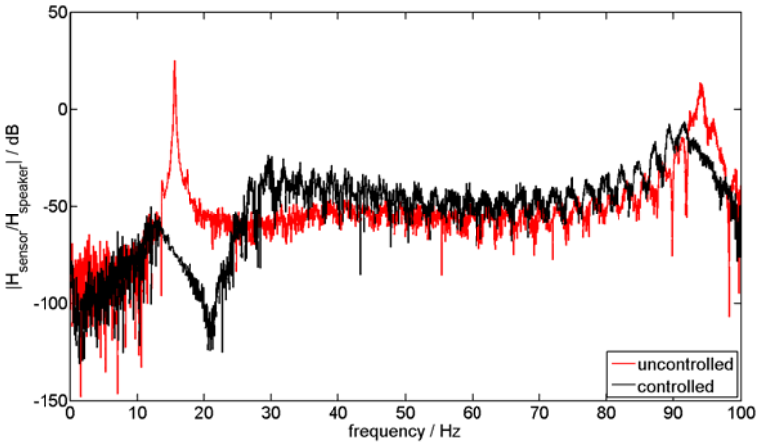

Figure 6: Bending angle on the tip measured by the sensor network

The same behaviour can be seen from the deflection signal of the laser sensor.

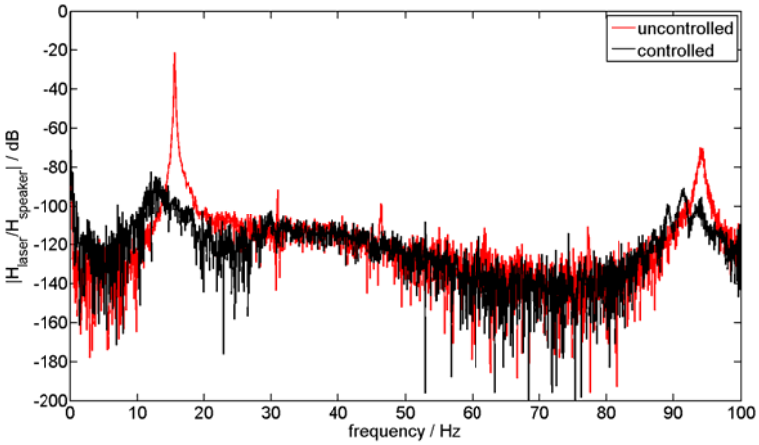

Figure 7: Deflection of the tip measured by the laser sensor

9. CONCLUSION

In this paper we have presented the implementation of a wireless communication system to a strain measurement structuralmonitoring approach of mechanical systems. Given a three storey frame structure, we take a closer look at one elastic member of the frame structure, comprising three piezoelectric sensors. For this simplified scenario a wireless communication system was established and the main design questions regarding sampling rate and latency were investigated and corresponding results are presented. For future work the implementation of the elastic member including the proposed control scheme in the three storey frame structure is planned. Also several requirements for the WCS have to be investigatedin more detail. On the one hand the bidirectional communication between sensor node and base node, for driving the actuator network wireless, has to be established. On the other hand the software stack from Texas Instruments lacks synchronization capabilities. Therefore, we plan to exchange the network stack with other protocols like proposed in (Berger et. al. 2012) and to integrate the system in a closed-loop system.

ACKNOWLEDGEMENT

Support of the authors from the COMET K2 – Austrian Center of Competence in Mechatronics (ACCM) is gratefully acknowledged.

REFERENCES

Berger, A., Potsch, A. and Springer, A. (2012), “Real-time data collection in a spatially extended TDMA-based wireless sensor network”, Proceedings of the 6th IEEE Topical Conference on Wireless Sensors and Sensor Networks, WiSNet

Chadwick, P. (1976), Continuum mechanics concise theory and problems, George Allen &Unwin, London, 1976

Gaudenzi, P. and Facchini, G. (2013), ”Wireless Structural Sensing”, Selected, peer reviewed papers from the VI Eccomas Thematic Conference on Smart Structures and Materials, SMART13, 155-165, Torino

Hackmann, G., Guo, W., Yan, G. et al (2010), “Cyber-physical Codesign of Distributed Structural Health Monitoring with Wireless Sensor Networks.”, Proceedings of the 1st ACM/IEEE International Conference on Cyber-Physical Systems, ICCPS '10

Huber, D. (2011), “Modeling and control of thin plate structures by piezoelectric actuators and sensors”, TraunerVerlag

Irschik, H., Krommer, M., Belyaev, A. K. and Schlacher, K. (1999), “Shaping of Piezoelectric Sensors/Actuators for Vibrations of Slender Beams: Coupled Theory and Inappropriate Shape Functions”, Int. J. of Intelligent Materials Systems and Structures, **9**, 546-554

Irschik, H., Krommer, M. and Pichler, U. (2003), “Dynamic shape control of beam-type structures by piezoelectric actuation and sensing“, International Journal of Applied Electromagnetics and Mechanics, **17**, 251-258

Irschik H. and Nader, M. (2009), “Actuator placement in static bending of smart beams utilizing Mohr’s analogy”, Engineering Structures, **31**, 1698-1706

Kim S., Pakzad S., Culler D. et al (2007), “Health Monitoring of Civil Infrastructures Using Wireless Sensor Networks,” Proceedings of the 6th International Conference on Information Processing in Sensor Networks, IPSN

Krommer, M. (2001), “On the correction of the Bernoulli-Euler beam theory for smart piezoelectric beams”, Smart Materials and Structures, **10**(4), 668-680

Krommer, M. and Nader, M. (2004), “Collocated actuator/sensor design for shape control of sub-regions of structures”, Proc. of SPIE’s 11th Annual International Symposium on Smart Materials and Structures, Smith, R., ed., **5383**, 232-243

Krommer, M. and Zellhofer, M. (2010), “Monitoring and control of multi-storey frame structures by strain-type actuators and sensors“, in Mechanics and Model-Based Control of Smart Materials and Structures, Springer, New York, Vienna, 115-124

Kugi A. (2001), Non-linear control based on physical methods, Springer, London

Miu, D. K. (1993), Mechatronics: Electromechanics and Contromechanics, Springer, New York

Pin, N. and Zhihua, J. (2010), “Requirements, challenges and opportunities of wireless sensor networks in structural health monitoring”, Proceedings of the 3rd IEEE International Conference on Broadband Network and Multimedia Technology, IC-BNMT

Tauchert, T. R. (1992), “Piezothermoelastic behaviour of a laminated plate”, Journal of Thermal Stresses, 25-37

Ziegler, F. (1998), Mechanics of Solids and Fluids, Springer, New York, Vienna